On the Control of Single Stage Centrifugal Compressor Surge with Active Magnetic Bearings

Se Young Yoon* and Zongli Lin
Dept. of Electrical and Computer Engineering
University of Virginia
Charlottesville, VA 22904, U.S.A.

Paul E. Allaire
Dept. of Mechanical and Aerospace Engineering
University of Virginia
Charlottesville, VA 22904, U.S.A.

Abstract

This paper presents a comprehensive step-by-step description of how to design and implement an Active Magnetic Bearing (AMB) based compressor surge controller, including experimental control results to demonstrate the effectiveness of the given approach. First, we provide a complete description of the industrial-size compressor test rig with AMBs that was specifically built for this study. Next, a detailed derivation of the dynamic equations describing the compressor flow is presented. The compressor model is later used in the synthesis of the model-based surge controller algorithm, which is implemented in the compressor test rig and tested experimentally. Illustrative details of the controller design, implementation, and testing are included.

1 Introduction

Centrifugal compressors are subject to flow instabilities. Among these instabilities, the most dominant is the phenomenon known as surge. Flow instability is a critical factor that limits the performance of compressors. If the performance of a compressor is pushed beyond the stability limit, the pressure build-up initiates unstable limit cycles in the flow that can damage the compressor and other attached system components [1]. Indeed, the flow oscillations during the surge limit cycle can cause extensive damage to the compressor casing and internal components due to the high vibration loads [2]. Because the economic loss due to surge damage in compressors can be significant, there have been continual efforts by the academic and industrial communities to find a reliable and efficient solution.

The most common approach to dealing with compressor surge is surge avoidance. The majority of current compressors are operated conservatively to avoid surge, trading achievable pressure head for stability robustness. In surge avoidance a flow margin is implemented between the minimum allowed output flow and the predicted surge initiation point, which acts as a safety buffer in case external disturbances perturb the compressor operation towards instability. There is a trade-off between stability and performance, because a large surge margin limits the operating range of the compressor. In the situation when external flow disturbances push the compressor operating point into the instability region of surge, a reset mechanism releases the pressure build-up in the system and brings the compression system back to stability.

An alternative option to surge avoidance is to implement an active surge control mechanism that stabilizes the compressor flow, effectively extending the operational range of the compressor with no loss in performance [3]. In active control, flow actuators attempt to maintain the flow condition in a small neighborhood of the equilibrium operating point based on measurements from pressure and/or flow sensors. The implementation of such a controller has, however, been limited in industrial applications, mostly because successful experimental demonstration has been limited to very few special cases. Many surge control schemes require special actuators and important customization of the system components.

*syy5b@virginia.edu

Active magnetic bearings (AMBs) are increasingly used in compressors due to the low maintenance requirements and small parasitic energy losses [4]. Recently, promising results have been obtained for an active surge control scheme in a test rig, which modulates the impeller axial position to stabilize the flow in AMB-supported single stage centrifugal compressors [5, 6, 7]. Using the thrust AMBs as a high bandwidth actuator to regulate the impeller axial displacement, the compressor flow is restored to the equilibrium operating point during the early stages of the surge instability. Experimental data demonstrated that this surge control method is able to extend the stable flow range by more than 21% from the uncontrolled surge point.

In this paper we present an overview description of how to design and implement the AMB based compressor surge controller from our experience with the compressor surge test rig described in [7]. The more detailed technical aspect of the results reviewed in this paper can be found in [8, 6, 7]. This paper also includes experimental control results to demonstrate the effectiveness of the presented approach. First, we provide in Sect. 2 a complete description of the industrial-size compressor test rig with AMBs that was specifically built for this study. Next, a detailed derivation of the equations describing the compressor flow dynamics is presented in Sect. 3. The compressor model is later used in Sect. 4 for the synthesis of the model-based surge control algorithm, which is implemented in the compressor test rig and tested. Experimental surge control results are presented in Sect. 5. Insight views and details of the controller design, implementation, and testing process are included.

2 Experimental Compressor Test Rig

An industrial-size centrifugal compressor test rig was built by the Rotating Machinery and Controls Laboratory (ROMAC) at the University of Virginia. Figure 1 shows the compressor together with the inlet and the exhaust piping. The compressor is a single-stage centrifugal machine that operates with an unshrouded impeller and a vaneless diffuser. The diameter of the 18-blade unshrouded impeller is 250 mm, and the blade height at the tip is 8.21 mm. The nominal impeller tip clearance is 0.6 mm. At an operating speed of 23,000 rpm, the compressor is designed for an output nominal flow rate of 0.833 kg/s and pressure ratio of 1.68. The compressor components of this test rig was manufactured and donated to us by Kobe Steel.

The bearing housing shown in Fig. 2 holds a set of radial active magnetic bearings (AMBs) and a thrust AMB. The magnetic bearing levitates the rotor within the bearing clearances, providing the necessary support and damping for high speed operation. The thrust AMB also controls the axial position of the impeller, which allows to modify in real time the axial clearance between the impeller blade tip and the static shroud. For the control of surge, we will exploit this extra capability of the thrust AMB to perturb the flow through the compressor and counteract the unstable dynamics of surge. The range of the impeller axial displacement is limited by the backup bearing of the thrust AMB to ± 0.254 mm.

The layout of the compressor test rig is illustrated in Fig. 3. The compressor takes air from the atmosphere, and the pressurized output gas is returned back to the atmosphere after passing through the exhaust piping. High bandwidth pressure and temperature sensors are installed along the inlet and exhaust pipes following the PTC-10 code for compressors [9]. The locations of these sensors along the piping system is shown in Fig. 3. The mass flow through the compression systems is measured using an orifice flow meter, which is installed at the return section of the exhaust pipe. Orifice flow meters are only reliable for steady state measurements, thus it is only used for system characterization and not for control purposes.

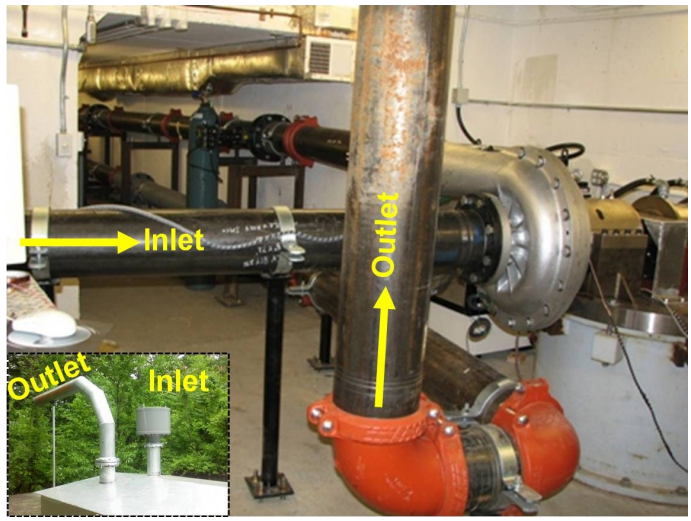

Figure 1: Photograph of the compressor with inlet and exhaust piping.

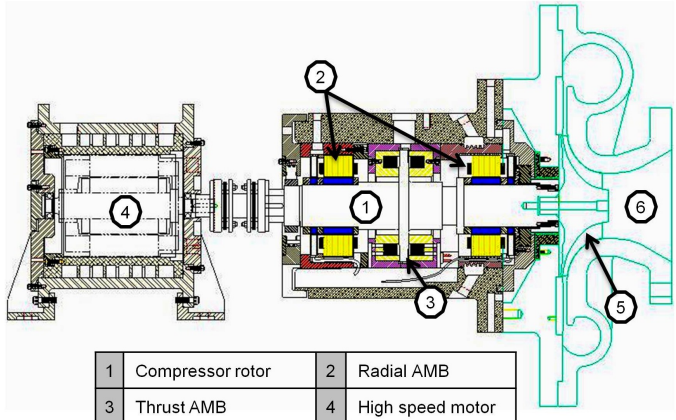

1	Compressor rotor	2	Radial AMB
3	Thrust AMB	4	High speed motor
5	Unshrouded impeller	6	Inlet

Figure 2: Drawing of the single stage centrifugal compressor with AMBs.

3 Compressor Surge Modeling and Actuator Characterization

First of all, the compressor steady state operation is characterized experimentally. For the compressor test rig presented in Sect. 2, we need to map the characteristic curve and the load curve of the system. The measured compressor characteristic curve for the compressor test rig is shown in Fig. 4. The surge region in the characteristic curve is in the low-flow/high-pressure area of the figure, where the flow becomes unstable and steady state measurements can not be obtained.

The downstream load in the compression system is controlled by the throttle valve, and the output flow is a function of the throttle valve percentage opening and the pressure in the throttle duct. In steady state operation, a load curve of pressure vs. flow-rate can be mapped by varying the throttle valve opening within the allowed range for the hardware. The characteristic curve and the

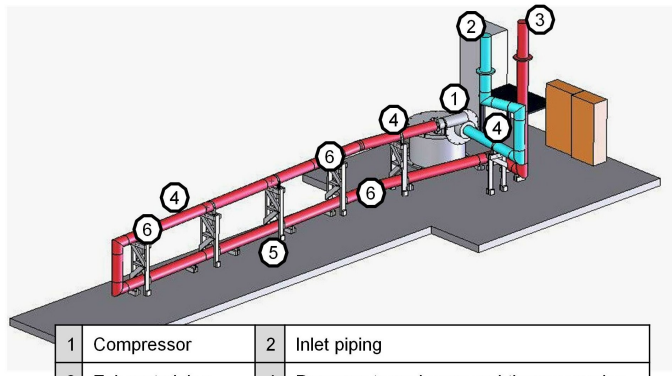

1	Compressor	2	Inlet piping
3	Exhaust piping	4	Pressure transducers and thermocouples
5	Orifice flow meter	6	Throttle valve positions

Figure 3: Layout of the compressor test rig, where the throttle valve can be installed at 2.2 m, 7.1 m or 15.2 m along the exhaust pipe.

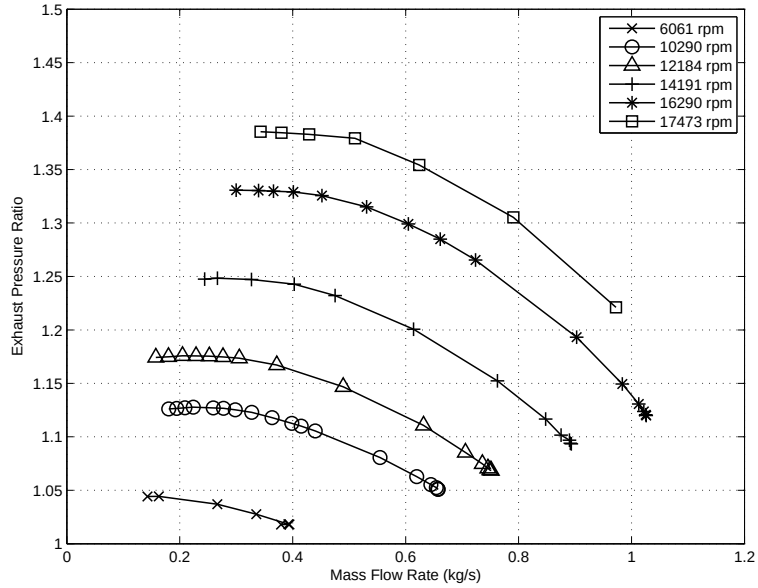

Figure 4: Compressor characteristic curves at different operating speeds

load curve are important to determine the equilibrium operating point of the compression system. The intersecting point of these two curves is where the stable compressor should operate at in terms of pressure and flow rate. Based on the computed equilibrium point, the surge controller designed in this paper will attempt to maintain the output of the system within a small neighborhood of the equilibrium values.

The surge instability model used in this study is the Greitzer two-state lumped parameter model developed in [10]. The Greitzer model describes a compression system composed by the compressor, the plenum volume collecting the compressed gas, and the throttle valve controlling the flow at

the plenum output. The states of this simplified one dimensional flow model are the non-dimensional compressor mass-flow rate Φ_c and the non-dimensional plenum pressure rise Ψ_p. Under the assumptions on the system flow condition and component geometry as listed in [10], the state equations of the Greitzer model are found to be

$$\dot{\Phi}_c = B\omega_H\left(\Psi_c - \Psi_p\right), \tag{1a}$$

$$\dot{\Psi}_p = \frac{\omega_H}{B}\left(\Phi_{th} - \Phi_p\right). \tag{1b}$$

The nondimensionalization of the states is standard in compressor applications, and it is described in [10]. The expression for the compressor pressure rise Ψ_c will be discussed later as we introduce the actuation on the impeller tip clearance to the model. The constants B and ω_H are the Greitzer stability constant and the Helmholtz frequency, respectively. The first value described the stability characteristics of the compression system, and the latter contains information on the resonance frequency of the flow. Lastly, the mass flow rate through the throttle duct is given by Φ_{th}, which is computed from the throttle pressure rise Ψ_{th}, throttle percentage opening u_{th} and throttle valve constant c_{th} as

$$\Phi_{th} = u_{th}c_{th}\sqrt{\Psi_{th}}. \tag{2}$$

The introduction of the variation in the impeller tip clearance as a perturbation to the compressor surge dynamics was first studied in [11]. The original expression derived in [11] was corrected in [5] based on experimental observation. The corrected expression for the compressor pressure rise as a function of the impeller tip clearance variation δ_{cl} is,

$$\Psi_c = \Psi_{c,ss} + \frac{p_{o1}}{\frac{1}{2}\rho_{o1}U^2}k_{cl}\delta_{cl}, \tag{3}$$

where $\Psi_{c,ss}$ is the compressor steady state pressure, and it is obtained from the fitted characteristic curve as a function of Φ_c,

$$\Psi_{c,ss} = A_1\Phi_c^3 + B_1\Phi_c^2 + D_1. \tag{4}$$

Other constants in (3) are the system inlet density ρ_{o1} and inlet pressure p_{o1}, the impeller tip speed U, and the tip clearance constant k_{cl}. The values of these constants can be found in [7].

For systems with long exhaust and inlet piping, the modes added by the acoustic resonance in the ducting system can affect the dynamics of surge. For the compression system in Sect. 2, it was observed from experimental surge measurements that the instability is initiated by the loss of damping in the piping acoustic modes. Since the original Greitzer model does not capture the acoustic modes in the piping system, the dynamics of the piping is introduced by incorporating a modal approximation of the transmission line model between the the compressor and the plenum equations in (1). The states of the pipeline equations are the throttle pressure rise Ψ_{th} and the plenum mass flow rate Φ_p, and the assembled total system equations are given as,

$$\dot{\Phi}_c = B\omega_H\left(A_1\Phi_c^3 + B_1\Phi_c^2 + D_1 + \frac{p_{o1}}{\frac{1}{2}\rho_{o1}U^2}k_{cl}\delta_{cl} - \Psi_p\right), \tag{5a}$$

$$\dot{\Psi}_p = \frac{\omega_H}{B}\left(\Phi_c - \Phi_p\right), \tag{5b}$$

$$\dot{\Psi}_{th} = \frac{2A_{12}A_c}{\rho_u U}\Phi_p + \frac{2B_{12}A_c}{\rho_u U}u_{th}c_{th}\sqrt{\Psi_{th}}, \tag{5c}$$

$$\dot{\Phi}_p = \frac{A_{21}\rho_u U}{2A_c}\Psi_{th} + A_{22}\Phi_p + B_{22}u_{th}c_{th}\sqrt{\Psi_{th}} + \frac{B_{21}\rho_u U}{2A_c}\Psi_p + \frac{\rho_u p_{o1}}{\rho_{o1}UA_c}\left(A_{21} + B_{21}\right). \tag{5d}$$

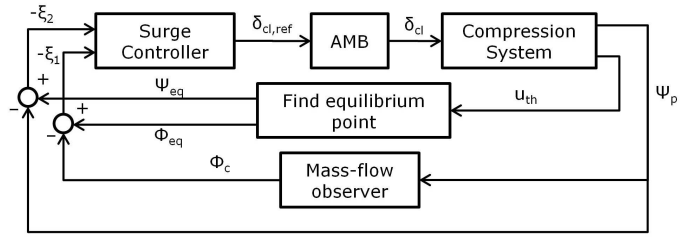

Figure 5: Surge controller feedback loop.

The constant A_{ij} and B_{ij} come from the derivation of the pipeline equations, and their values are given in [7]. Other constants in (5) are the pipeline upstream average density ρ_{u}, and the compressor duct cross-sectional area A_{c}.

4 Active Surge Control Law Design

The active surge control law is derived from the linearized expression of (5). The measured feedback signal to the controller is the plenum pressure rise Ψ_{p}, while the output of the controller is the commanded impeller tip clearance $\delta_{\mathrm{cl,ref}}$ to the thrust active magnetic bearing. The objective of the surge controller is to stabilize the compressor flow within a small neighborhood of the equilibrium flow condition. The linearized states of the compression system are defined as,

$$\xi_1 = \Phi_{\mathrm{c}} - \Phi_{\mathrm{eq}}, \tag{6}$$

$$\xi_2 = \Psi_{\mathrm{p}} - \Psi_{\mathrm{eq}}, \tag{7}$$

$$\xi_3 = \Psi_{\mathrm{th}} - \Psi_{\mathrm{eq}}, \tag{8}$$

$$\xi_4 = \Phi_{\mathrm{p}} - \Phi_{\mathrm{eq}}, \tag{9}$$

where Φ_{eq} and Ψ_{eq} are the equilibrium non-dimensional mass flow rate and pressure rise, respectively, where the system is linearized. The selection of the linearization point is crucial for the design of the surge controller. First of all, the linearization must be done in the unstable section of the characteristic curve in order to capture the surge dynamics. On the other hand, if the linearization point is selected too deep in the surge region, then the surge controller will overcompensate for the surge instability. This will result in a controller with a high bandwidth requirement and an output signal that is susceptible to saturation and noise transmission.

The feedback control loop implemented for the active surge controller is illustrated in Fig. 5. The information coming from the compressor is the plenum pressure rise and the throttle valve percentage opening, which is used to determine the equilibrium pressure and mass flow rate. The compressor mass flow rate is the third piece of information and it is estimated from the pressure rise signal by employing a nonlinear observer developed in [12]. The addition of the observer in the control loop reduces the transmission of sensor noises to the controller output as demonstrated in [12], which is crucial for applications with narrow actuator saturation limits such as the one presented in this paper.

The equations of the surge controller is synthesized using the H_∞ approach. The H_∞ synthesis method is well known in control theory, and its objective is to minimize the H_∞-norm of a generalized closed loop system [13]. Then, by adding frequency dependent weighting functions at the inputs and outputs of the system, the shape of the closed loop transfer function with the surge con-

troller can be manipulated. A detailed discussion on the synthesis of the H_∞ surge controller is presented in [7].

An important characteristic of the implemented controller that needs to be considered during the design stages is the unavoidable error between the reference impeller tip clearance $\delta_{\text{cl,ref}}$ in Fig. 5 coming from the controller, and the actual impeller tip clearance δ_{cl} observed by the compressor. The error between these two signals is introduced by the closed loop dynamics of the thrust AMB. Although the dynamics of the actuator is sometime considered as a simple bandwidth limitation as discussed in [14], it was shown in [8] that this approach is not sufficient to guarantee the stability of the compressor with the surge controller. In order to prove the stability of the closed loop compression system in Fig. 5, the robustness condition to the AMB dynamics needs to be added in the controller derivation as shown in [7]. Additionally, the levitation controller closing the control loop of the AMBs needs to be carefully designed to minimize the error between $\delta_{\text{cl,ref}}$ and δ_{cl}.

5 Experimental Testing

In this section we present experimental measurements that was obtained from the test rig described in Sect. 2 with the surge controller. The test speed for the compressor is 16,290 rpm, which was limited by the power electronics driving the motor. Additionally, in this initial experimental test, the size of the plenum volume is reduced by moving the throttle valve to the nearest location to the compressor.

The frequency response of the measured plenum pressure signal is shown in Fig. 6 for the base case with the surge controller unactivated. The figure shows how the frequency response of the plenum pressure signal changes as the throttle valve is gradually closed from 21% opening down to 16.5% opening. In the figure we also see two red dashed lines parallel to the throttle opening axis, corresponding to the system Helmholtz frequency at 8 hz and piping acoustics mode at 21 hz. A single dashed line parallel to the frequency axis indicates the valve opening percentage at the initialization of the surge instability. We observe in Fig. 6 that the first indication of the surge instability appears at 17.7% throttle opening, with the disturbances exciting the piping acoustic mode. As the throttle valve is further closed, the instability evolves to the full limit cycle with dominant frequency slightly below the Helmholtz frequency.

The same frequency response of the measured plenum pressure signal as in Fig. 6 is shown for the case with the surge controller activated in Fig. 7. In this case we clearly observe the effect of the surge controller, suppressing the unstable dynamics of surge and stabilizing the system pressure output for lower throttle openings. Eventually, a limit is reached where the surge controller cannot stabilize the flow anymore. This limit in the stability of the controlled system is expected, since the linearized model is only accurate within a neighborhood of the linearization values. The stability could be further improved in latter iterations by implementing a nonlinear surge controller. In the experimental test setup considered in this study, the stability limit with the surge controller is reached at 16.4% throttle opening.

The measured system steady state pressure and flow rate outputs are mapped in Fig. 8 together with the characteristic curve. When the surge controller is unactivated, the steady state operation can only be measured to the right of the surge limit at $\Phi = 0.14$. When the flow condition is pushed to the right of this limit, the compression system enters the surge limit cycle. On the other hand, when the surge controller is activated, we are able to push the surge limit by 21.3% and map a section of the positive slope region of the characteristic curve. This allows the compressor to operate safer at the peak pressure point with a large margin between the operating point and the surge limit.

Relevant system conditions during the surge control test are presented in Fig. 9. The figure shows, in the clockwise direction from the top-left, the throttle percentage opening u_{th}, the percent-

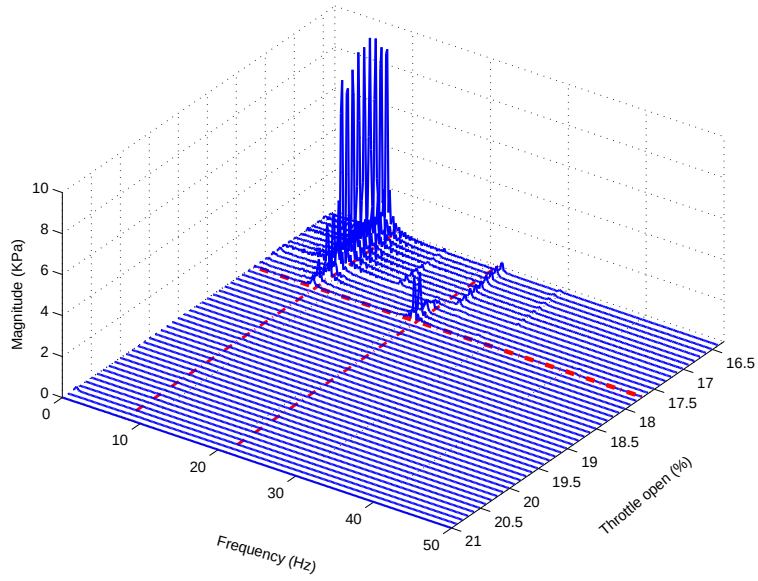

Figure 6: Frequency response of the measured plenum pressure signal with the surge controller unactivated as the compressor is driven into the surge region by closing the throttle valve opening.

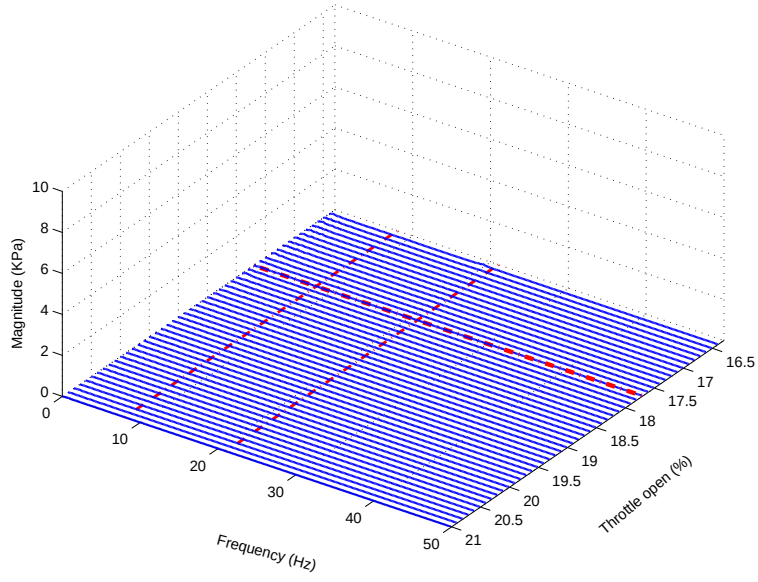

Figure 7: Frequency response of the measured plenum pressure signal with the surge controller activated as the compressor is driven into the surge region by closing the throttle valve opening.

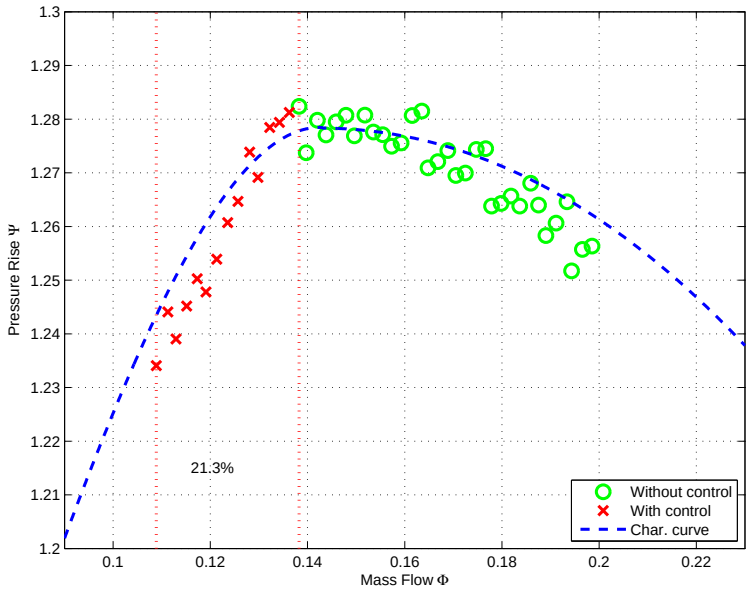

Figure 8: Measured steady state compressor operating points on the interpolated characteristic curve, corresponding to the system operating with the surge controller activated and unactivated.

age tip clearance modulation, linearized system states, and the non-dimensional plenum pressure rise Ψ_p. Figure 9 shows that the current iteration of the surge controller uses 60% of the available tip clerance, which is relatively high. However, we must keep in mind that the compressor would not operate constantly in surge condition, but the surge controller is only meant to be a short time solution to external disturbances momentarily pushing the system into the surge region.

6 Conclusions

A comprehensive insight on the design and implementation of the AMB based compressor surge controller was presented in this paper. Based on a compressor surge test rig with a AMB-supported single-stage unshrouded centrifugal compressor, this paper described the process of implementing the surge controller. Also, detailed information was provided on the importance of different components in the feedback loop for the success of the surge controller. The implemented surge controller was tested and experimental results were presented here. The mapped compressor characteristic curve with the surge controller activated demonstrated that the surge controller can extend the stability region of the compressor flow by 21.3%. This is significant when we consider that such benefits can be obtained almost for free in systems that already integrates AMBs.

References

[1] R. C. Pampreen. *Compressor Surge and Stall*. Concepts ETI, Vermont, USA, 1993.

[2] B. de Jager. Rotating stall and surge control: A survey. In *Proceedings of the 34th IEEE Conference on Decision and Control*, pages 1857–1862, 1995.

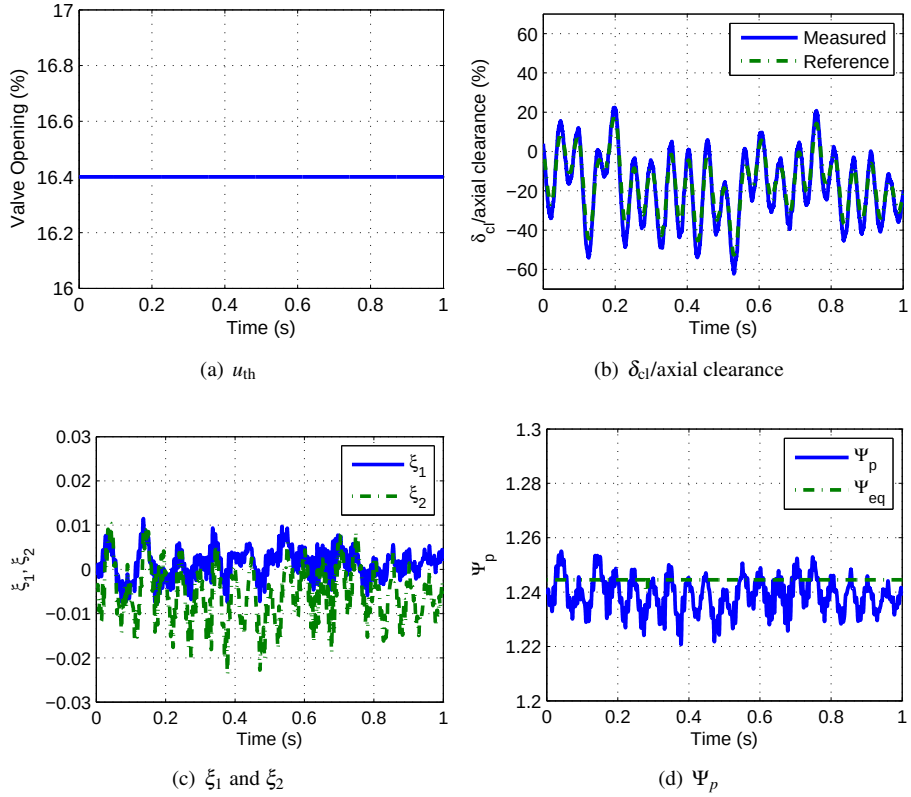

(a) u_{th} (b) δ_{cl}/axial clearance

(c) ξ_1 and ξ_2 (d) Ψ_p

Figure 9: Experimental surge control test at 16,290 rpm

[3] A. H. Epstein, E. Ffowcs Williams, and E. M. Greitzer. Active suppression of aerodynamic instabilities in turbomachinery. *Journal of Propulsion and Power*, 5:204–211, March 1989.

[4] G. Schweitzer and E. H. Maslen, editors. *Magnetic Bearings*. Springer, 2009.

[5] S. Y. Yoon, Z. Lin, K. T. Lin, and P. Allaire. Compressor surge control with amb actuation. In *The Eleventh International Symposium on Magnetic Bearings*, August 2008.

[6] S. Y. Yoon, Z. Lin, C. Goyne, and P. E. Allaire. An enhanced greitzer compressor model including pipeline dynamics and surge. *ASME Journal of Vibration and Acoustics*, 133:051005 (14), 2011.

[7] S. Y. Yoon, Z. Lin, and P. E. Allaire. Design and implementation of a surge controller for an amb supported compressor in the presence of piping acoustics. In *Proceedings of the 50th IEEE Conference on Decision and Controls*, dec 2011.

[8] S. Y. Yoon, Z. Lin, K. T. Lim, C. Goyne, and P. E. Allaire. Model validation for an amb-based compressor surge control test rig. *ASME Journal of Vibration and Acoustics*, 132:061005 (13), 2010.

[9] American Society of Mechanical Engineers, New York, NY. *PTC-10: Performance Test Code on Compressors and Exhausters*, 1997.

[10] E. M. Greitzer. Surge and rotating stall in axial flow compressors, part i, ii. *ASME Journal of Engineering for Power*, 120:190–217, 1976.

[11] D. Sanadgol. *Active Control of Surge in Centrifugal Compressors Using Magnetic Thrust Bearing Actuation*. PhD thesis, University of Virginia, 2006.

[12] S. Y. Yoon, Wei Jiang, Z. Lin, and P. E. Allaire. Flow-rate observers in the suppression of compressor

surge using active magnetic bearings. In *Proceedings of ASME Turbo Expo 2012*, jun 2012.

[13] L. Lublin, S. Grocott, and M. Athans. h_2 (lqg) and h_∞ control. In *The Control Handbook*, pages 651–661. CRC Press, Inc., 1996.

[14] J. S. Simon, L. Valavani, A. H. Epstein, and E. M. Greitzer. Evaluation of approaches to active compressor surge stabilization. *ASME Journal of Turbomachinery*, 115:57–67, January 1993.